Article

The Lyotropic Nature of Halates: An Experimental Study

Mert Acar [1] **, Duccio Tatini** [1] **, Barry W. Ninham** [2,3] **, Federico Rossi** [4] **, Nadia Marchettini** [4] **and Pierandrea Lo Nostro** [1,*]

1   Department of Chemistry "Ugo Schiff" and CSGI, University of Florence, 50019 Firenze, Italy
2   Materials Physics (Formerly Department of Applied Mathematics), Research School of Physics, Australian National University, Canberra, ACT 2600, Australia
3   School of Science, University of New South Wales, Northcott Drive, Campbell, Canberra, ACT 2612, Australia
4   Department of Earth, Environmental and Physical Sciences, University of Siena, 53100 Siena, Italy
*   Correspondence: pierandrea.lonostro@unifi.it; Tel.: +39-055-4573010

Abstract: Unlike halides, where the kosmotropicity decreases from fluoride to iodide, the kosmotropic nature of halates apparently increases from chlorate to iodate, in spite of the lowering in the static ionic polarizability. In this paper, we present an experimental study that confirms the results of previous simulations. The lyotropic nature of aqueous solutions of sodium halates, i.e., $NaClO_3$, $NaBrO_3$, and $NaIO_3$, is investigated through density, conductivity, viscosity, and refractive index measurements as a function of temperature and salt concentration. From the experimental data, we evaluate the activity coefficients and the salt polarizability and assess the anions' nature in terms of kosmotropicity/chaotropicity. The results clearly indicate that iodate behaves as a kosmotrope, while chlorate is a chaotrope, and bromate shows an intermediate nature. This experimental study confirms that, in the case of halates XO_3^-, the kosmotropic–chaotropic ranking reverses with respect to halides. We also discuss and revisit the role of the anion's polarizability in the interpretation of Hofmeister phenomena.

Keywords: Hofmeister series; kosmotropicity; chaotropicity; halates; chlorate; bromate; iodate; polarizability

1. Introduction

Specific ion or Hofmeister effects consist of the change of a measurable property induced in a particular system when an electrolyte is added, a change that can be often ranked according to a sequence that is commonly referred to as the "Hofmeister series" [1–3].

Hofmeister effects are not accounted for by classical theories of electrolytes, electrochemistry, or colloid and surface science. These theories, developed before quantum mechanics, rely only on electrostatic forces between ions and between ions and surfaces. The series differ from substrate to substrate, depending also on the solvent and on polarity and hydrophobicity of interfaces [4]. The phenomena are observed usually (but not always) when the concentration of the salt is greater than 10 mM, where quantum mechanical forces dominate electrostatics [5]. This concentration threshold is commonly reached everywhere in biology and nearly everywhere else. We recall that, originally, dispersion forces are referred to as electromagnetic fluctuation forces at visible frequencies [6]. However, in the *continuum* solvent model, electromagnetic forces include all fluctuation frequencies, from zero to microwave, including collective dipolar, infrared, visible, far UV, and X-ray regions.

While the inclusion of dispersion with electrostatic forces provides the basis for an inclusive framework to accommodate most ion specific phenomena, the whole story is more complicated, and, as we will later see, hydration is a central player [7].

There are no systems where specific ion effects do not occur, from bulk solutions, pH, buffers, activities, zeta and surface and membrane potentials, ion pumps, enzymatic action, and oscillating reactions [8]; from inorganic to organic and biochemical systems; or from aqueous media to nonaqueous solvents [9,10]. The literature on this topic is vast, and the

interested reader can refer to the cited works and references therein [9–12]. Yet, there is no universal behavior to trace Hofmeister phenomena, i.e., in some cases, the series reverses, and in other cases, some differences in the expected order can be found. Often anions are more effective than cations [9].

In order to attempt to quantify and explain the observed specific ion effects, the experimentalist may find it useful to plot the results as a function of some ion-specific physico-chemical parameters (which we will call *descriptors*) that reflect the nature of the ions, their behavior in hydration, adsorption at interfaces, and more often, in general, in solution, under the (usually omitted) assumption that the contribution of the cation and of the anion are independent and additive. This well-established procedure has two advantages: (i) it allows one to demonstrate and quantify the occurrence of a Hofmeister phenomenon [7,13] and (ii) it helps to trace the mechanism and effect of the investigated ions in a particular case [14]. Among these descriptors, the most common include the ionic static polarizability (α) [15], the surface tension molar increment (k_1) [16], the lyotropic number (*N*) [17], the Gibbs free energy and entropy of hydration ($\Delta_{\mathrm{hydr}}G$ and $\Delta_{\mathrm{hydr}}S$, respectively) [18,19], the entropy change of water (calculated as the difference between the partial molar entropy of the ion and that of a water molecule surrounded by the other solvent molecules, ΔS_{II}) [20], and the Jones-Dole viscosity coefficient (B_{JD}) [21].

More literature references and an extensive discussion on these descriptors can be found in Refs. [7,9].

Each descriptor and other physico-chemical parameters are related to the specific nature of the ions, i.e., to their hydration properties, adhesion to interfaces, and interactions with specific sites. We recall that Hofmeister phenomena occur also in nonaqueous and aprotic solvents, where hydrogen bond clusters do not exist, but van der Waals and quadrupolar interactions play a significant role in setting the solvent structure [22–24]. This fact has important consequences on several phenomena, for instance, in the stabilization of a protein's conformation, solubility, and functionalities, and in industrial fermentation processes [25].

The terms chaotropic and kosmotropic, frequently used in specific ion effect studies, refer to the supposed capability of an ion or a molecule to modify the "water structure" [26]. In fact, according to this hypothesis, when an ion enters a bulk water phase, it first perturbs the hydrogen-bonding network and the structure of water molecules in the liquid state. Then, the powerful ion's electric field around a small and strongly hydrated kosmotrope will have a great impact on the permanent dipole moment of the surrounding water molecules and force a higher order on local water molecules mainly via charge-dipole interactions. On the other hand, the large and poorly hydrated chaotropes, surrounded by a much weaker electrostatic field, will not offset the original perturbation in the water structure and leave the nearby water molecules more disordered with respect to the pure liquid reference. In other words, the strength of the water-water interactions in the bulk phase can be taken as a reference to distinguish between kosmotropes (where ion-water interactions are stronger than water-water interactions) and chaotropes (where ion-water interactions are weaker than water-water interactions) [9]. This effect is thought to take place also in the case of some neutral molecules, such as sugars [27].

Beyond the terms, the concepts related to kosmotropicity and chaotropicity are still debated in the literature [28], for example, in relation to the salting-in and salting-out effects that salts induce in proteins and other macromolecules in water depending on their concentration [29–31].

More recent investigations on cellular activities, on the origin of life on Earth, and on the possibility of extraterrestrial life confirm how strong the implications of these phenomena are [32–35].

Using the words of Ball and Hallsworth, we can state that "chaotropicity might function as one such empirically defined "black box" term that can help us to classify and organize our thinking while acknowledging that at a deeper, mechanistic level, the story is more complex and not so easily compartmentalized" [36]. In other words, far from

implying a real, detectable, and measurable water structure, the terms kosmotrope and chaotrope are to be used as a rule of thumb [36], useful to identify the nature of a solute and describe its effects in a particular system.

Usually, kosmotropic ions possess low polarizabilities due to their high charge density, high surface tension molar increments, very high free energies of hydration, and definitely positive Jones-Dole viscosity coefficients. On the other hand, chaotropes possess large polarizabilities (that implies their electronic clouds are very sensitive to external electric fields), lower surface tension molar increments, small free energies of hydration, and negative Jones-Dole viscosity coefficients.

Concerning halides, their free energy of hydration decreases from $F^- > Cl^- > Br^- > I^-$. This trend perfectly reflects the strong kosmotropicity of fluoride and the strong chaotropicity of iodide with chloride and bromide somewhere in between.

On the other hand, the opposite trend is found for the halates, XO_3^-, where X = Cl, Br, or I. Based on its polarizability, iodate should behave like thiocyanate or iodide, i.e., like strong chaotropes. Instead, its properties, e.g., the thermodynamic functions of hydration, are typical of a strong kosmotrope [1].

The basic theoretical features of density, viscosity, refractive index, conductivity are reported in Appendix A.

In this paper, we report on the experimental values of density, viscosity, refractive index, and conductivity of sodium halates in water in order to investigate their nature in terms of kosmotropicity vs. chaotropicity and to compare our conclusions with the evidence given by previous computational studies [37–39].

Finally, we will revisit and discuss the role of polarizability, one of the most important descriptors of Hofmeister phenomena, in the case of halates.

2. Results and Discussion

The experimental results for the three halates at different concentrations will be presented and discussed separately in the following order: density, viscosity, conductivity, and refractive index for the three halates.

2.1. Density

The density values at 20 °C, 25 °C, 30 °C, 35 °C, and 40 °C of sodium chlorate, bromate, and iodate in water as a function of the concentration are listed in Tables S1–S5 (see the Supplementary Material). The plots of ρ versus the molal concentration of the three salts at constant temperature are shown in Figures S1–S5 (see the Supplementary Information). At constant concentration and temperature, the density trend is always

iodate > bromate > chlorate

This suggests a kosmotropic behavior of IO_3^- and chaotropic nature for ClO_3^-, with BrO_3^- behaving in an intermediate manner.

The standard partial molar volumes $\overline{V}_2^0$ of each salt solution at 25 °C were calculated according to Equation (A4). They are listed in Table 1 and compared with those published by Millero [40]. The Masson's equation (Equation (A5)) was used to obtain the empirical S_V^* coefficients to gain insight on the solute-solute and solute-solvent interactions. In Figure 1, a linear fitting of the apparent molar volumes vs. the square root of the concentration is shown. Each salt has a positive slope, indicating the presence of solute-solute interactions, and with an increasing value of the slope (S_V^*) going from sodium chlorate (black circles) to iodate (red circles).

Table 1. Standard partial molar volumes $\overline{V}_2^o$ calculated according to Equation (A4) and compared with the values reported in Ref. [40], standard electrostrictive molar volumes $\overline{V}_{2,el}^o$ for each investigated salt at 25 °C expressed in (cm^3·mol^{-1}) according to Equation (A6), and S_V^* coefficients obtained by fitting the data according to Equation (A5).

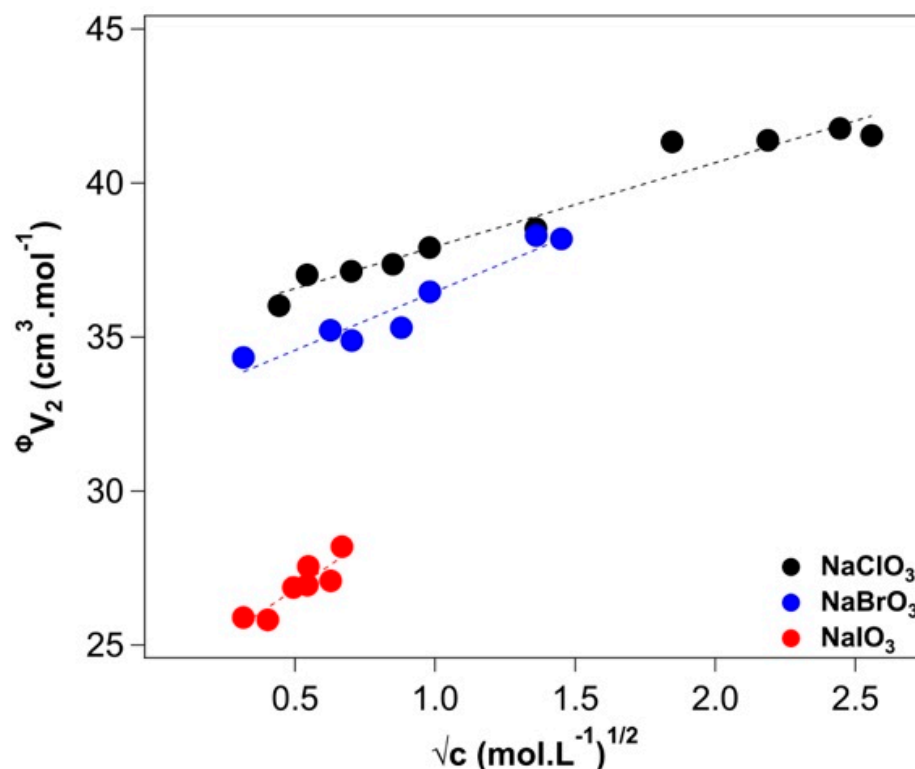| Salt	$\overline{V}_2^o$	$\overline{V}_2^o$ [40]	$\overline{V}_{2,el}^o$	$\overline{V}_{2,el}^o(\%)$	S_V^*
NaClO$_3$	35.7 ± 0.2	35.5	-9.4 ± 0.2	-21	2.7 ± 0.2
NaBrO$_3$	32.8 ± 0.2	34.1	-14.4 ± 0.2	-31	3.8 ± 0.5
NaIO$_3$	24.7 ± 0.3	24.1	-12.1 ± 0.3	-33	6.2 ± 1.3

Figure 1. Linear fitting of the Masson's equation (Equation (A5)). Sodium chlorate (black), bromate (blue), and iodate (red) solutions. The experimental error is $\pm 1\%$.

The S_V^* for iodate is three times larger than that of chlorate. This occurrence can be ascribed to the formation of ion pairs that, in the former, occur at lower concentration, as the conductivity and viscosity data will confirm (see below). This conclusion is in line with the Law of Matching Water Affinities that predicts the formation of stable ion pairs between ions that possess similar solvation features, i.e., when the cation and the anion are either both kosmotropic or chaotropic [41,42].

The standard electrostrictive molar volumes were calculated according to Equation (A6). For the intrinsic volumes of the ions in first approximation, we used the estimates from Padova [43], obtained by assuming that anions and cations in the solution keep the same coordination number they have in the crystal lattice. The results were normalized by dividing the electrostrictive molar volume by the intrinsic volume ($\overline{V}_{2,el}^o(\%)$) in order to compare ions of different sizes [44].

The standard partial molar volumes obtained at 20 °C, 30 °C, 35 °C, and 40 °C are listed in Table S6 (see the Supplementary Material). The values of $\overline{V}_2^o$ regularly increase with temperature for all salts.

2.2. Viscosity

The viscosity values are listed in Table S7 and plotted in Figure S6 (see the Supplementary Material). Equation (A8) was used to fit the data as a function of the salt concentration (see Figure 2). The *A* coefficients were calculated according to the Falkenhagen-Vernon equation [45,46]. The extracted fitting parameters are listed in Table 2.
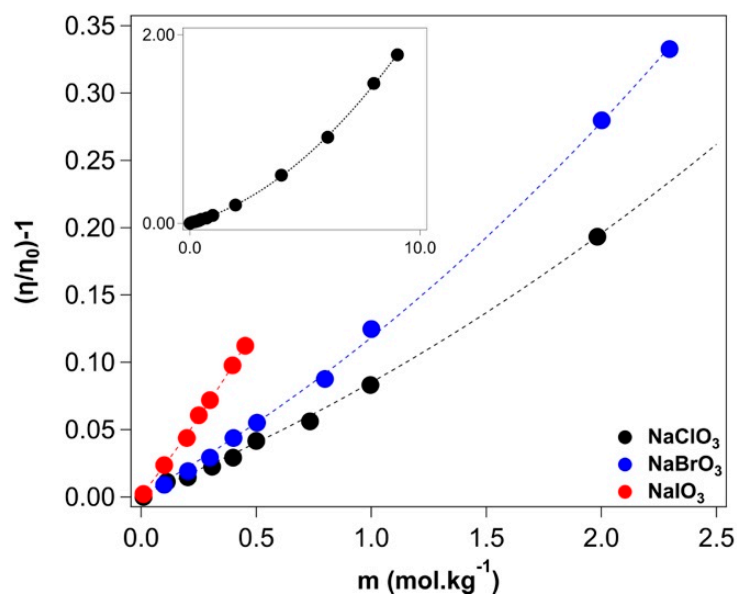

Figure 2. Extended Jones-Dole (Equation (A8)) fitting for sodium chlorate (black), bromate (blue), and iodate (red) solutions. The inset shows the values in the entire range of concentrations for sodium chlorate.

Table 2. *A* (in $mol^{-1/2} \cdot L^{1/2}$), B_{JD} (in $mol^{-1} \cdot L$), and *D* (in $mol^{-3/2} \cdot L^{3/2}$) coefficients obtained by fitting the data with Equation (A8). The B_{JD} values are compared with those reported by Ref. [21] and with those of sodium halide [21].

Halate	A	B_{JD}		D	Halide	B_{JD}
		This Work	**Ref. [21]**			**Ref. [21]**
NaClO$_3$	0.0066	0.064 ± 0.002	0.063	0.015 ± 0.001	NaCl	0.080
NaBrO$_3$	0.0071	0.089 ± 0.004	0.094	0.023 ± 0.002	NaBr	0.052
NaIO$_3$	0.0083	0.197 ± 0.008	0.225	0.089 ± 0.021	NaI	0.012

The B_{JD} coefficient increases progressively from sodium chlorate to bromate and iodate, which is consistent with a more kosmotropic nature of iodate, the opposite of that found for halides anions ($I^- < Br^- < Cl^- < F^-$), as shown in Table 2 [47].

Considering that the D coefficient is related to the ion-pairing effects that take place at relatively high concentrations of salts, we can conclude that sodium iodate has the highest propensity to form ion pairs with respect to sodium chlorate and bromate (see Table 2). This result will be confirmed by the results obtained from the conductivity measurements (see the next subsection).

2.3. Conductivity

Conductivities and molar conductivities of the salt solutions at different concentrations are listed in Tables S8 and S9 (see the Supplementary Information). Figure S7 shows the plot of the conductivity κ as a function of the molar concentration for the aqueous solutions of sodium chlorate, bromate, and iodate at 25 °C. As shown in Figure 3, the molar conductivity decreases faster for sodium iodate solutions than for sodium bromate and chlorate solutions.
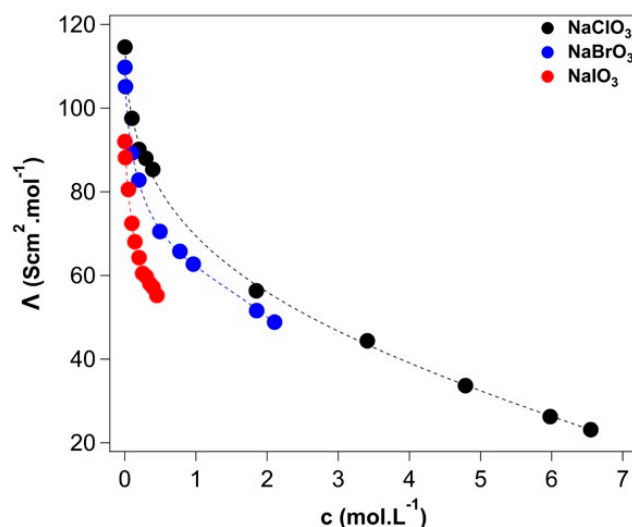
Figure 3. Molar conductivity Λ as a function of concentration (c, in molar units) of sodium chlorate (black), bromate (blue), and iodate (red) solutions. Dotted lines represent the fitting of Equation (A10). The experimental absolute error on the molar conductivity values is ± 0.1.

This behavior is related to the formation of ion pairs, which should be more relevant in the case of sodium iodate. In fact, from the $\Lambda/\sqrt{c_2}$ plot (see Figure S8 in the Supplementary Information), it appears that the linear dependence of the molar conductivity on the square root of the salt concentration holds until a concentration threshold is reached. After such a value, the conductivity of the solution is described by a more complex formula (Equation (A10)). A possible explanation of this behavior might be related to the formation of ion pairs. Roughly, this threshold is 0.25 M for $NaIO_3$, 0.38 M for $NaBrO_3$, and 0.49 M for $NaClO_3$. This result is in line with the tendency of these salts to form ion pairs and is confirmed by their solubilities in water, approximately 0.454 M for $NaIO_3$, 2.412 M for $NaBrO_3$, and 9.930 M for $NaClO_3$ at 20 °C, as discussed by Collins [48].

The limiting molar conductivities Λ^∞ were calculated from the molar conductivities according to Equation (A10) (see Table 3). From these, we obtained the mean ionic activity coefficient $\gamma_\pm$ (see Table S10 and Figure S9 in the Supporting Information) from Equation (A9). The data are compared with those available in the literature obtained by different methods, i.e., isopiestic method for sodium chlorate and bromate and vapor-pressure osmometry for sodium iodate (see Table S10 in the Supporting Information).

Table 3. Limiting molar conductivity (Λ^∞, in $S \cdot cm^2 \cdot mol^{-1}$) values at 25 °C of sodium chlorate, bromate, and iodate solutions obtained from the fitting of Equation (A10) and from Ref. [49].

Salt	This Work	Ref. [49]
$NaClO_3$	116.51 ± 0.74	114.68
$NaBrO_3$	112.22 ± 0.36	105.78
$NaIO_3$	91.98 ± 0.98	90.58

The Trusdell-Jones equation (Equation (A11)) was used to fit the mean ionic activity coefficients to extract the linear, ion-specific b parameter, positive for kosmotropes and negative for chaotropes. For chlorate and bromate, b is approximately -0.02 dm^3/mol, while for iodate it has a positive value of 0.11 dm^3/mol. As in the case of the viscosity, B_{JD} coefficient:

$$IO_3^- > BrO_3^- > ClO_3^-$$
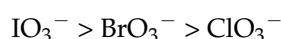
with a progressive lowering in the kosmotropic character of the ion.

2.4. Refractive Index and Polarizability

The refractive index values, measured at 20 °C, are listed in Table S11 (see the Supplementary Information). Figure 4 shows the concentration dependence of the refractive index for the three sodium halates in water. On the *x*-axis, the concentration is expressed in g.mL^{-1} because these are the units used in the calculation (Equation (A12)).
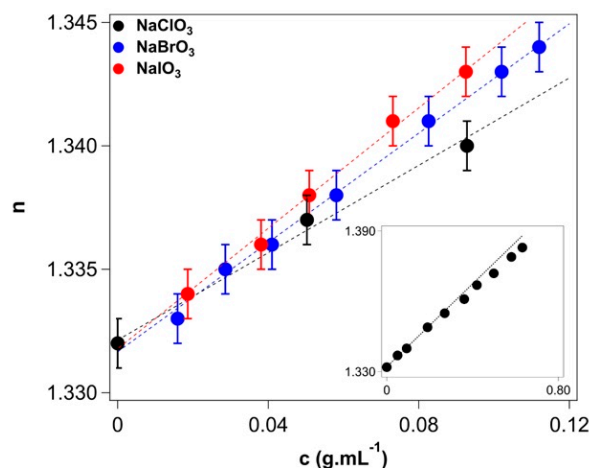

Figure 4. Refractive index values at 20 °C as a function of the concentration of sodium chlorate (black), bromate (blue), and iodate (red) solutions. Dotted lines represent the linear fitting according to Equation (A12). The inset shows the measured refractive index for the entire range of concentration for sodium chlorate investigated in this work.

The values of α that we extracted from Equation (A13) and listed in Table 4 show that the most polarizable ion is iodate, reflecting the greater number of electrons in iodine and, therefore, the extension and softness of its electronic cloud. A smaller polarizability is usually thought to reflect a strong kosmotropic nature of the ion. This is the case, for instance, for Li$^+$ and F$^-$ [48]. Within the halide group, α increases significantly from F$^-$ to I$^-$ because of (1) the increasing number of electrons in the anion and (2) the progressively weaker attraction between the nucleus and the electrons in the external orbitals due to the shielding effect of the more numerous inner electrons. This implies that the electronic cloud in iodide is more expanded (actually the polarizability is expressed in terms of a volume) and softer, i.e., the compactness of the cloud is more sensitive to an external electric field. Finally, the polarizability is a very important ion-specific parameter because it appears in the equations that describe the strength of dispersion (London) and induction (Debye) forces [9]: the larger α, the stronger the interactions between an ion or a molecule and its counterpart. These interactions are always attractive, and given the fact that anions possess larger polarizabilities, anions often (but not always) induce stronger Hofmeister effects than do cations [9].

Table 4. Refractive indices (n_{salt}) obtained from Equation (A12), and polarizabilities (α, in Å^3) obtained from Equation (A13) compared with the literature values.

Salt	n_{salt}	α	A [a]
NaClO$_3$	1.553 ± 0.007	5.40 ± 0.06	5.23 (5.43)
NaBrO$_3$	1.702 ± 0.007	6.94 ± 0.05	6.47 (6.49)
NaIO$_3$	1.854 ± 0.009	8.22 ± 0.07	8.01 (7.64)

[a] Polarizability values calculated using the experimental values for halate anions from Ref. [50] and for the sodium ion from Ref. [51]. The values in parentheses were calculated using the theoretical polarizability of halate anions from Ref. [52].

On the basis of these premises, we conclude here that the meaning and relevance of polarizability in the framework of Hofmeister phenomena need to be revisited. In fact, kosmotropes are usually referred to as ions with low polarizability, large free energy and

entropy of hydration, large surface tension molar increments, positive values of the Jones-Dole B coefficient, and small or even negative partial molar volumes (see Tables 2 and 5). Chaotropes are just the opposite.

Table 5. Anion radius (r, in nm), hydration shell thickness (Δr, in nm), and number of water molecules in the hydration shell (n). Free energy change ($\Delta_{hydr}G$) and entropy change ($\Delta_{hydr}S$) of hydration, lyotropic number (N), molar surface tension increment (k_1) and entropy change of water (ΔS_{II}).

Ion	r [a]	Δr [a]	n [a]	$\Delta_{hydr}G$ [a]	$\Delta_{hydr}S$ [b]	N [c]	k_1 [d]	ΔS_{II} [e]
Na^+	0.102	0.116	3.5	−365	−111	100	1.20	−5.4
ClO_3^-	0.200	0.033	1.8	−280	−80	10.65	0.00	5.0
BrO_3^-	0.191	0.038	1.9	−330	−95	9.55	0.35	−5.0
IO_3^-	0.181	0.043	2.0	−400	−148	6.25	0.70	(−47)

[a] From Ref. [18]; [b] from Ref. [19]; [c] from Ref. [17]; [d] from Ref. [14]; and [e] from Ref. [20].

The results obtained in this work show that within the halates XO_3^- series, IO_3^- is the most kosmotropic species, and ClO_3^- is the most chaotropic. This is the conclusion that can be drawn on the basis of the density, viscosity, and conductivity data.

Instead, the polarizability of the three salts decreases from iodate to chlorate, conflicting with the common opinion that kosmotropes are supposed to possess lower polarizabilities than chaotropes.

It is not simply a matter of shape or of polyatomic ions, as all halates have a pyramidal structure [38,39] and contain one halogen occupying the pinnacle and three oxygens at the base of the pyramid, with a residual negative charge. Instead, the real significant player is hydration. In fact, Table 5 shows that the main hydration parameters are greater for iodate and smaller for chlorate.

It is important to consider all possible solvation sites in a polyatomic ion to obtain a better picture of the overall behavior of the solutes in the Hofmeister series [39]. Finally, we observe that the polarizability of the anion, obtained from the experimental refractive indices of its aqueous solutions, does not match with its lyotropic nature. Instead, it is the presence of an electron-richer and more polarizable atom, such as iodine, that gives rise to the "cationic character" in these polyatomic ions [38,39].

In the end, the electronegativity difference between oxygen and the halogen atom and the structure of halates result in the formation of an asymmetric charge distribution and, thus, in an internal dipole that eventually modifies the interactions of the ion with the solvent [38,39] and defines its kosmo- or chaotropic nature.

2.5. Results from Previous Molecular Dynamics Studies

Molecular dynamics and density functional theory studies, confirmed by multi-edge X-ray adsorption fine structure spectroscopy measurements [38], revealed two strongly hydrated regions in the iodate ion that bear opposite charges: the first is around the iodine atom and bears a formally positive charge, whereas the latter encompasses all oxygen atoms and possesses a formally negative charge [38]. The charge separation is due to the electronegativity difference between I (2.66) and O (3.44).

This particular asymmetry in the charge distribution of the iodate ion is thought to be responsible for the peculiar behavior toward the solvating water molecules. Apparently, the positive region is strongly hydrated by three water molecules with a staggered orientation with respect to the oxygens of IO_3^-, whilst approximately nine waters hydrate the negative region where the three oxygens are located (see Figure 5). Moreover, the water molecules that surround the positive region are oriented in the "lone pair" position typical of a hydrated cation, with a tilted water dipole moment to allow for the lone pairs to have a direct interaction with the cation [38].
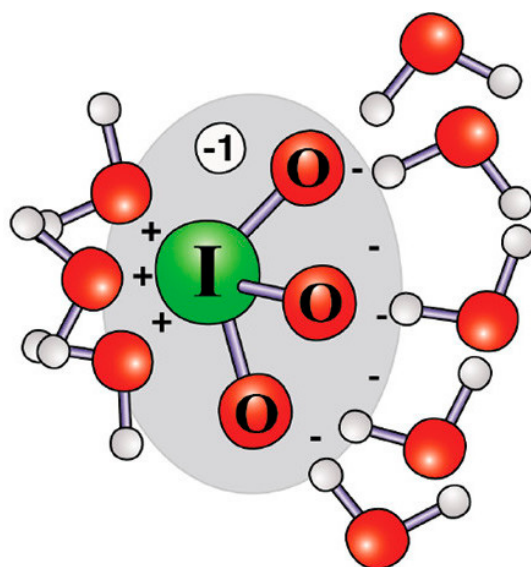
Figure 5. Schematic representation of an IO_3^- ion surrounded by hydrating water molecules in the two regions that bear positive (left) and negative (right) charges. Reprinted with permission from Ref. [38]. Copyright 2011 American Chemical Society.

Another computational study investigated the bromate ion/water system in a quantum density functional theory (DFT) framework, examining the solvation shell structure and dynamics [39]. In this case, the interaction of the water molecules with the positively charged bromine produces only a "shoulder" region in the radial distribution function, and not a well-defined hydration shell, as in the case of iodate. The "shoulder" region of water molecules appears to have a preference for a 120° orientation so that the lone pairs of the water's oxygens can interact favorably with the positively charged bromine. In general, the dynamics occur faster at the "shoulder" region, while those at the solvation shell region possess a slower dynamic compared with the bulk. Interestingly in the "shoulder" region, water molecules have a slower diffusion compared with the bulk. This was ascribed to the fact that although water molecules have fast escape time scales, once they move close to the oxygens, they form hydrogen bonds and do not move away from the ion [39]. To the best of our knowledge, no molecular dynamics simulations have been performed on the chlorate ion.

Table 5 reports the anion radius, hydration shell thickness, and number of water molecules in the hydration shell, as reported by Marcus [18].

In spite of the larger size of iodine respect to bromine and chloride, the halate ions' dimension increases the opposite way. In conclusion, iodate is more compact than chlorate. This can also be related to the greater propensity of iodine to establish double bonds with oxygen, a feature that decreases in bromine and chlorine. The number of water molecules in the hydration shell (n in Table 5) reported by Marcus, instead, does not change significantly from one ion to another.

3. Materials and Methods

Milli-Q water from Millipore with a resistivity of 18.2 MΩ·cm and a conductivity of 0.055 μS·cm^{-1} was used. $NaClO_3$, $NaBrO_3$, and $NaIO_3$ were purchased from Acros Organics (with a declared purity of 99%, 99+%, and 99%, respectively). The solutions were prepared by weighing the salts and water, and the concentrations were expressed in molal units. For data analysis, where needed, the molal concentrations were transformed to molar concentrations using the density values obtained in this work.

Density measurements ($\pm 5 \cdot 10^{-6}$ g·cm^{-3}) were conducted with an Anton-Paar$^©$ DMA 5000 density meter. All measurements were carried out at five different temperatures: 20 °C, 25 °C, 30 °C, 35 °C, and 40 °C (± 0.001 °C) as a function of the salt concentration.

An Ubbelohde viscometer with a capillary diameter of 0.36 ± 0.01 mm from Schott (Mainz, Germany) was used. All measurements were conducted at 25 °C in a water bath equipped with an immersion thermostat Lauda E200 comprising a Pt-100 temperature probe that is used for measuring the actual temperature with an accuracy of ± 0.01 °C. Each solution was equilibrated for 30 min before performing the viscosity measurement. The flow time (t) was measured by a stopwatch (± 0.01 s). and was converted to the solution viscosity (in cP) by $\eta = A\rho t$, as t is always larger than 200 s [53]. The A constant was calculated using the tabulated value for pure water at 25 °C (0.89040 cP). The viscosity was determined as a function of the salt concentration at constant temperature for the three sodium halates.

The conductivity meter was purchased from Hach, model senIon^{TM}+ EC7 (Lainate, Italy), which operates with an error lower than 0.1% for the conductivity values and lower than 0.2% for the temperature control.

During the experiments, two different probes were used due to the high difference in conductivity values between MilliQ water and the salt solutions. The probes were also purchased from Hach (models sensIon^{TM}+ 50 70 with a range from 0.2 µS/cm to 200 mS/cm, and sensIon^{TM}+ 50 71 with a range from 0.05 µS/cm to 30 mS/cm). All measurements were carried out at 25 °C.

An Abbé refractometer model NAR-1T LIQUID from Atago Italia Srl (Milan, Italy) was used for the refractive index measurements ($\pm$ 0.0002 nD). The Abbé refractometer was connected to a water bath. All measurements were carried out at 20 °C.

4. Conclusions

This work, on the basis of the measurements of density, conductivity, refractive index, and viscosity of sodium halates (chlorate, bromate, and iodate) aqueous solutions, pinpoints that iodate is a strong kosmotropic ion, while bromate and chlorate possess a chaotropic nature. This is precisely the reversed trend that the spherical and monoatomic halides show, where iodide is the most chaotropic anion and fluoride is the most kosmotropic.

The salt polarizability, obtained from refractive index data, is larger for iodate and smaller for chlorate. This is a very interesting result, as this parameter is a classic descriptor in specific ion effect studies. In fact, kosmotropes, e.g., fluoride or lithium, possess the lowest values of polarizability, whereas chaotropes, such as iodide or cesium, show the largest values of polarizability. With this work, we show that, at least in the case of halates, this correlation does not hold. These data confirm what previous computational studies concluded [38,39]. A deep analysis of the electronic and structural features of the anions suggests that their lyotropic nature is determined basically by their hydration properties which, in turn, depend on the presence of an internal dipole in the ion due to the different electronegativity and size of the halogen atom.

In the near future, we will address this topic for other series of anions in order to highlight the relevance of their size, shape, and electronegativity in their properties and in the effects they produce in solution.

Supplementary Materials: The following supporting information can be downloaded at: https://www.mdpi.com/article/10.3390/molecules27238519/s1, Table S1 and Figure S1: Density (ρ, in g·cm^{-3}) at 20 °C of sodium chlorate, sodium bromate, and sodium iodate solutions at different concentrations (m, in molal units); σ is the standard deviation, Table S2 and Figure S2: Density (ρ, in g·cm^{-3}) at 25 °C of sodium chlorate, sodium bromate, and sodium iodate solutions at different concentrations (m, in molal units); σ is the standard deviation, Table S3 and Figure S3: Density (ρ, in g·cm^{-3}) at 30 °C of sodium chlorate, sodium bromate, and sodium iodate solutions at different concentrations (m, in molal units); σ is the standard deviation, Table S4 and Figure S4: Density (ρ, in g·cm^{-3}) at 35 °C of sodium chlorate, sodium bromate, and sodium iodate solutions at different concentrations (m, in molal units); σ is the standard deviation, Table S5 and Figure S5: Density (ρ, in g·cm^{-3}) at 40 °C of sodium chlorate, sodium bromate, and sodium iodate solutions at different concentrations (m, in molal units); σ is the standard deviation, Table S6: Standard partial molar volumes ($\overline{V}_2^o$, in cm^3·mol^{-1}) at 20 °C, 25 °C, 30 °C, 35 °C, and 40 °C for sodium chlorate, bromate,

and iodate, Table S7 and Figure S6: Viscosity (η, in cP) at 25 °C of sodium chlorate, bromate, and iodate solutions at different concentrations (m, in molal units); σ indicates the standard deviation, Table S8 and Figure S7: Conductivity (κ, in μS·cm^{-1}) at 25 °C of sodium chlorate, bromate, and iodate solutions at different concentrations (c, in molar units); σ is the standard deviation, Figure S8: Molar conductivity (Λ, in S·cm^2·mol^{-1}) at 25 °C for sodium chlorate, sodium bromate, and sodium iodate solutions as a function of the square root of the concentration c (in molar units), Table S9: Molar conductivity (Λ, in S·cm^2·mol^{-1}) at 25 °C for sodium chlorate, sodium bromate, and sodium iodate solutions at different concentrations (c, in molar units); σ is the standard deviation, Table S10 and Figure S9: Mean ionic activity coefficients ($\gamma_{\pm}$) at 25 °C of sodium chlorate, sodium bromate, and sodium iodate solutions as a function of the concentration (c, in molar units) obtained by using Equation (A9) [54,55]; the error is of 1.3%, 0.6%, and 2.1% for sodium chlorate, bromate, and iodate, respectively, Table S11: Refractive index (n) at 20 °C of sodium chlorate, bromate, and iodate solutions at different concentrations (c, in molar units and c*, in g·mL^{-1}); σ is the standard deviation.

Appendix A

Appendix A.1. Density

The density ρ of electrolyte solutions is strictly related to the nature of the dissolved ions and of the solvent [56,57]. From ρ, the standard partial molar volume $\overline{V}_2^o$ of a solute can be obtained. The latter depends on the solute-solvent interactions [21,44,58]. Electrostriction, i.e., the partial molar volume change of the solvent with concentration, is ion-specific [44] and can be very effective, as the electric pressure exerted by an ion on the nearby water molecules can be as high as hundreds of MPa and, thus, may produce a significant lowering in the solvent volume, depending on the specific ions and on their concentration [44,56]. At higher electrolyte concentrations this effect reaches a plateau because of the charge screening effect. Polarization and electrostriction of solvent molecules are not simply due to the Coulombic terms in ion-water interactions but also depend on the dispersion interactions that, in turn, depend on the ionic polarizability [59,60]. Hence, electrostriction and partial molar volumes uncover specific ion effects.

For a multicomponent solution, the partial molar volume of each species i is defined as [61]:

$$\overline{V}_i = \left(\frac{\partial V}{\partial n_i}\right)_{T,p,n_{j\neq i}} \tag{A1}$$

where V and n_i are the solution volume and the number of moles of i, respectively. In this work, we consider only binary solutions and will use the indices 1 and 2 to indicate the solvent and the solute, respectively.

$\overline{V}_2^o$ can be obtained from the density measurements by calculating the apparent molar volume $^{\Phi}\overline{V}_2$, i.e., the molar volume of the solute when the solvent volume is taken as that of the pure solvent [62]:

$$^{\Phi}\overline{V}_2 = \frac{1000(\rho^* - \rho)}{m_2 \rho \rho^*} + \frac{M_2}{\rho} \tag{A2}$$

where ρ^* and ρ are the densities of the pure solvent and of the solution (in $g \cdot cm^{-3}$), respectively, at the same temperature, m_2 is the solute concentration in molal units, and M_2 is the molar mass of the solute (in $g \cdot mol^{-1}$). $^{\Phi}\overline{V}_2$ is expressed in $cm^3 \cdot mol^{-1}$.

According to the Redlich, Rosenfeld, and Meyer's (RRM) model [57,62], the apparent molar volume depends on the square root of the concentration:

$$^{\Phi}\overline{V}_2 = \overline{V}_2^o + S_V^{DH}\sqrt{c_2} \tag{A3}$$

where S_V^{DH} derives from the Debye-Hückel model; it is the same for ions bearing the same charge and depends only on the solvent and temperature [57]. We recall that Equation (A3), which is valid for dilute solutions, is based on pure electrostatics.

The dependence on $\sqrt{c_2}$ is typical of electrostatics-based models, such as in the Debye-Hückel theory for activity coefficients, the viscosity of a salt solution, and conductivity. When the system is fairly dilute, e.g., roughly below 1 mM, all salts with the same stoichiometry behave in the same way, and there is no room for specificity.

For higher concentrations, a further term in c_2 is needed to best fit the data [57]:

$$^{\Phi}\overline{V}_2 = \overline{V}_2^o + S_V^{DH}\sqrt{c_2} + b_V c_2 \tag{A4}$$

The same occurs for the aforementioned parameters: for dilute solutions of strong electrolytes, the average ionic coefficient, the molar conductivity, and the viscosity of the solution are well described by the extended Debye-Hückel, the Kohlrausch, and the Jones-Dole equations, respectively. For small concentrations, the term in $\sqrt{c_2}$ prevails and electrostatic models apply. For moderate to high concentrations, the ion-specific term in c_2 dominates. Equation (A4) can also be expressed using an empirical S_V^* coefficient instead of S_V^{DH}, which is the case of the Masson's equation [40,57]:

$$^{\Phi}\overline{V}_2 = \overline{V}_2^o + S_V^*\sqrt{m} \tag{A5}$$

where the concentration is expressed in molal units and is the starting point of the RRM model. Negative slopes indicate ideal mixing of the solute with the solvent, with no solute-solute interactions, while positive slopes reflect the presence of non-negligible solute-solute interactions, as, for example, in ion pair formation [63–65].

The standard electrostrictive molar volume $\overline{V}_{2,el}^o$ is calculated using the intrinsic molar volume of the electrolyte $\overline{V}_{2,intr}$, which cannot be obtained from experiments [44]. The literature offers different approaches to estimate the intrinsic molar volume, for example, those of Marcus and Pedersen [66,67] and Padova [43].

Equation (A6) is used to obtain the electrostrictive molar volumes [44]:

$$\overline{V}_{2,el}^o = \overline{V}_2^o - \overline{V}_{2,intr} \tag{A6}$$

where $\overline{V}_{2,el}^o$ and $\overline{V}_2^o$ refer to the same parameters at infinite dilution, i.e., where only ion-solvent interactions take place while ion-ion interactions are negligible [44]. Since the electrostrictive volume depends on the ion size, it must be normalized in order to compare the values for different ions. This can be accomplished by dividing the electrostrictive values by the intrinsic volumes of the salts, as suggested by Mazzini and Craig: $\overline{V}_{2,el}^o(\%) = 100\frac{\overline{V}_{2,el}^o}{\overline{V}_{2,intr}}$ [44].

$\overline{V}_{2,el}^o(\%)$ is a dimensionless parameter that normalizes electrostriction assuming that all electrolytes possess the same intrinsic molar volume, with no change in charge density,

polarizability, shape, etc.; $\overline{V}^o_{2,el}(\%)$ is zero when no electrostriction takes place, negative when it occurs, and positive when the solvent expands rather than contracting [44]. Since kosmotropic anions usually are small in size and possess small polarizabilities, they are expected to bring about the largest electrostriction [44]. Interestingly, strong kosmotropes, such as NaF, induce a strong electrostriction at all concentrations, while chaotropes, such as NaSCN, begin with a negative electrostriction volume, but then, at very high concentrations, the solvent expands as the water structure is destroyed.

Appendix A.2. Viscosity

This parameter is related to the measurement of the drag of the ionic atmosphere in the solution that causes the retardation of the ions' motion [68]. The Jones-Dole equation relates the viscosity η of a solution (with respect to that of the pure solvent at the same temperature, η_0) to the solute concentration c as [21,69]:

$$\frac{\eta}{\eta_o} - 1 = A\sqrt{c} + B_{JD}c \tag{A7}$$

At moderate-to-high concentrations the first term is negligible, and the second term, which reflects ion specificity and the onset of non-electrostatic interactions, dominates [9]. The coefficient A is roughly equal for ions with the same electric charge [21].

For $0.05 < c < 0.1$ M, the Jones-Dole equation holds [41,42,70], but for more concentrated solutions, above 0.5 M and up to 5 M, a quadratic term Dc^2 must be added to fit the experimental data [21,71,72]:

$$\frac{\eta}{\eta_o} - 1 = A\sqrt{c} + B_{JD}c + Dc^2 \tag{A8}$$

A difficulty is that even for the bulk solvent model and pure electrostatics, the Debye-Hückel behavior does not hold for multivalent ions or mixtures thereof at any reasonable concentration [73–75].

The Jones-Dole B_{JD} coefficient is an empirical fitting parameter, strictly dependent on the nature of the solute [13,21,76]. In fact, B_{JD} is positive for kosmotropes that are supposed to strengthen the local order of water and negative for chaotropes that partly break apart the structure of water and make it more fluid than bulk water at the same temperature [9]. It is assumed that the B_{JD} coefficients of cations and anions are additive [21] and that the contribution of each ion does not depend on the presence of the other ions. D is still poorly understood and presumably relates to solute-solute association (e.g., ion pairing) effects [72]. We recall that the terms "kosmotrope" and "chaotrope" refer to the effect of an ion on the structuredness of liquid water; the coefficient B_{JD} reflects the ordering induced by kosmotropes and the disordering created by chaotropes on water, a phenomenon that was already discussed by Poiseuille in 1847 [77], although, already in 1840, Dalton had observed that "certain anhydrous salts do not increase the volume of water on solution", perhaps one of the first experimental evidences of specific salt effects [78].

Appendix A.3. Conductivity

The conductivity measurements were used here to estimate the mean ionic activity coefficients, according to the Tamamushi equation [76,79,80]:

$$log\gamma_\pm = -\frac{A^*|z_+z_-|}{\alpha^*\Lambda^\infty + \beta^*(z_+ + |z_-|)}(\Lambda^\infty - \Lambda) \tag{A9}$$

where Λ is the molar conductivity of the electrolyte, and A^*, α^*, and β^* are fitting parameters [79]. This equation holds when the concentration is lower than 0.1 M, i.e., in the electrostatic regime [79]. To calculate the mean ionic activity coefficients, the values of limiting molar conductivities (Λ^∞) are needed. There are several equations that relate the molar conductivity to the salt concentration. They all derive from limiting laws that

account for the electrostatic Coulombic forces between the ions at dilute concentrations and that scale as $\sqrt{c}$ [76,81–83]. The Fuoss-Hsia equation and its modified Fernandez-Prini and Justice version are the most used equations [82,83]:

$$\Lambda = \Lambda^\infty - S\sqrt{c} + Ec \cdot ln(c) + J_1 c - J_2 c^{3/2} \tag{A10}$$

where S and E are related to the charge, mobility of the ions, and to the dielectric constant and viscosity of the solvent. J_1 and J_2 are specific to each electrolyte and include the ionic distance of closest approach. All these equations assume a complete dissociation of the salts; however, we recall that at higher concentrations, ion pairing occurs and modifies the conductivity of the solution [41,42].

The mean ionic activity coefficients can be expressed using the extended Debye-Hückel equation that contains a linear term in I, and the Truesdell-Jones b coefficient reflects the specific nature of the intervening ions [74,84,85]:

$$\log \gamma_\pm = -\frac{A|z_+ z_-|\sqrt{I}}{1 + Ba\sqrt{I}} + bI \tag{A11}$$

where z_+ and z_- are the charges of the cation and of the anion, respectively, I is the ionic strength ($I = \frac{1}{2}\sum_i c_i z_i^2$), A is a purely electrostatic coefficient, B is the reciprocal of the Debye screening length (i.e., the thickness of the ionic atmosphere), and a is the mean distance of nearest approach of the ions [86]. Both A and B depend on temperature and on the dielectric constant of the solvent. The numerator accounts for the long-range Coulombic forces, while the denominator shows how these are perturbed when the ions approach at a short distance, under the assumption that ions behave as non-deformable hard spheres. This assumption is not correct at higher concentrations, where the overcrowding of ions leads to non-negligible short-range attractive van der Waals interactions and to the vanishing of electrostatic forces. The b coefficient of the linear term in I precisely accounts for these non-electrostatic, ion specific interactions. Its introduction in the extended Debye-Hückel formula already appeared more than 60 years ago in the seminal book of Robinson and Stokes [76], but its physical meaning was elucidated only more recently, after the introduction of dispersion forces in the description of the interactions that determine the physical chemistry of electrolyte solutions. The treatment becomes more complicated in the case of unsymmetric electrolytes, for example, $CaCl_2$ (1:2) [73].

Appendix A.4. Refractive Index

The refractive index of a salt n_{salt} can be obtained using the De Feijter equation [87,88]:

$$\frac{dn}{dc} = \frac{1}{\rho_{salt}}(n_{salt} - n_{water}) \tag{A12}$$

where dn/dc is the refractive index increment calculated by fitting the refractive index values of salt solutions vs. the solute concentration.

The Lorentz-Lorenz formula calculates the salt polarizability α_{salt} from the refractive index values as [88,89]:

$$\alpha_{salt} = \frac{3}{4\pi N_A}\left(\frac{n_{salt}^2 - 1}{n_{salt}^2 + 2}\right)V_m \tag{A13}$$

where N_A is the Avogadro number, and V_m is the molar volume of the salt.

References

1. Gregory, K.P.; Elliott, G.R.; Robertson, H.; Kumar, A.; Wanless, E.J.; Webber, G.B.; Craig, V.S.J.; Andersson, G.G.; Page, A.J. Understanding Specific Ion Effects and the Hofmeister Series. *Phys. Chem. Chem. Phys.* **2022**, *24*, 12682–12718. [CrossRef] [PubMed]
2. Salis, A.; Ninham, B.W. Models and Mechanisms of Hofmeister Effects in Electrolyte Solutions, and Colloid and Protein Systems Revisited. *Chem. Soc. Rev.* **2014**, *43*, 7358–7377. [CrossRef] [PubMed]
3. Bruce, E.E.; Okur, H.I.; Stegmaier, S.; Drexler, C.I.; Rogers, B.A.; van der Vegt, N.F.A.; Roke, S.; Cremer, P.S. Molecular Mechanism for the Interactions of Hofmeister Cations with Macromolecules in Aqueous Solution. *J. Am. Chem. Soc.* **2020**, *142*, 19094–19100. [CrossRef] [PubMed]
4. Schwierz, N.; Horinek, D.; Netz, R.R. Anionic and Cationic Hofmeister Effects on Hydrophobic and Hydrophilic Surfaces. *Langmuir* **2013**, *29*, 2602–2614. [CrossRef] [PubMed]
5. Ninham, B.W.; Yaminsky, V. Ion Binding and Ion Specificity: The Hofmeister Effect and Onsager and Lifshitz Theories. *Langmuir* **1997**, *13*, 2097–2108. [CrossRef]
6. Yaminsky, V.V.; Ninham, B.W. Hydrophobic force: Lateral enhancement of subcritical fluctuations. *Langmuir* **1993**, *9*, 3618–3624. [CrossRef]
7. Tatini, D.; Ciardi, D.; Sofroniou, C.; Ninham, B.W.; Lo Nostro, P. Physicochemical Characterization of Green Sodium Oleate-Based Formulations. Part 2. Effect of Anions. *J. Colloid Interface Sci.* **2022**, *617*, 399–408. [CrossRef]
8. Budroni, M.A.; Rossi, F.; Marchettini, N.; Wodlei, F.; Lo Nostro, P.; Rustici, M. Hofmeister Effect in Self-Organized Chemical Systems. *J. Phys. Chem. B* **2020**, *124*, 9658–9667. [CrossRef]
9. Lo Nostro, P.; Ninham, B.W. Hofmeister Phenomena: An Update on Ion Specificity in Biology. *Chem. Rev.* **2012**, *112*, 2286–2322. [CrossRef]
10. Mazzini, V.; Craig, V.S.J. Volcano Plots Emerge from a Sea of Nonaqueous Solvents: The Law of Matching Water Affinities Extends to All Solvents. *ACS Cent. Sci.* **2018**, *4*, 1056–1064. [CrossRef]
11. Lo Nostro, P.; Lo Nostro, A.; Ninham, B.W.; Pesavento, G.; Fratoni, L.; Baglioni, P. Hofmeister Specific Ion Effects in Two Biological Systems. *Curr. Opin. Colloid Interface Sci.* **2004**, *9*, 97–101. [CrossRef]
12. Lonetti, B.; Lo Nostro, P.; Ninham, B.W.; Baglioni, P. Anion Effects on Calixarene Monolayers: A Hofmeister Series Study. *Langmuir* **2005**, *21*, 2242–2249. [CrossRef]
13. Salis, A.; Pinna, M.C.; Bilaničová, D.; Monduzzi, M.; Lo Nostro, P.; Ninham, B.W. Specific Anion Effects on Glass Electrode pH Measurements of Buffer Solutions: Bulk and Surface Phenomena. *J. Phys. Chem. B* **2006**, *110*, 2949–2956. [CrossRef] [PubMed]
14. Lagi, M.; Lo Nostro, P.; Fratini, E.; Ninham, B.W.; Baglioni, P. Insights into Hofmeister Mechanisms: Anion and Degassing Effects on the Cloud Point of Dioctanoylphosphatidylcholine/Water Systems. *J. Phys. Chem. B* **2007**, *111*, 589–597. [CrossRef] [PubMed]
15. Pyper, N.C.; Pike, C.G.; Edwards, P.P. The Polarizabilities of Species Present in Ionic Solutions. *Mol. Phys.* **1992**, *76*, 353–372. [CrossRef]
16. Marcus, Y. Individual Ionic Surface Tension Increments in Aqueous Solutions. *Langmuir* **2013**, *29*, 2881–2888. [CrossRef]
17. Voet, A. Quantative Lyotropy. *Chem. Rev.* **1937**, *20*, 169–179. [CrossRef]
18. Marcus, Y. Thermodynamics of solvation of ions. Part 5.—Gibbs free energy of hydration at 298.15 K. *J. Chem. Soc. Faraday Trans.* **1991**, *87*, 2995–2999. [CrossRef]
19. Marcus, Y. The Hydration Entropies of Ions and Their Effects on the Structure of Water. *J. Chem. Soc. Faraday Trans.* **1986**, *82*, 233–242. [CrossRef]
20. Krestov, G.A. *Thermodynamics of Solvation: Solution and Dissolution, Ions and Solvents, Structure and Energetics*; Ellis Horwood: New York, NY, USA, 1991.
21. Jenkins, H.D.B.; Marcus, Y. Viscosity B-coefficients of ions in solution. *Chem. Rev.* **1995**, *95*, 2695–2724. [CrossRef]
22. Collins, K.D.; Washabaugh, M.W. The Hofmeister Effect and the Behaviour of Water at Interfaces. *Q. Rev. Biophys.* **1985**, *18*, 323–422. [CrossRef]
23. Mazzini, V.; Craig, V.S.J. Specific-Ion Effects in Non-Aqueous Systems. *Curr. Opin. Colloid Interface Sci.* **2016**, *23*, 82–93. [CrossRef]
24. Sarri, F.; Tatini, D.; Tanini, D.; Simonelli, M.; Ambrosi, M.; Ninham, B.W.; Capperucci, A.; Dei, L.; Lo Nostro, P. Specific Ion Effects in Non-Aqueous Solvents: The Case of Glycerol Carbonate. *J. Mol. Liq.* **2018**, *266*, 711–717. [CrossRef]
25. Timson, D.J. The roles and applications of chaotropes and kosmotropes in industrial fermentation processes. *World J. Microbiol. Biotechnol.* **2020**, *36*, 89. [CrossRef]
26. Marcus, Y. Effect of Ions on the Structure of Water: Structure Making and Breaking. *Chem. Rev.* **2009**, *109*, 1346–1370. [CrossRef]
27. Edelman, R.; Kusner, I.; Kisiliak, R.; Srebnik, S.; Livney, Y.D. Sugar stereochemistry effects on water structure and on protein stability: The templating concept. *Food Hydrocoll.* **2015**, *48*, 27–37. [CrossRef]
28. Leontidis, E. Chaotropic salts interacting with soft matter: Beyond the lyotropic series. *Curr. Op. Coll. Interface Sci.* **2016**, *23*, 100–109. [CrossRef]
29. Zangi, R. Can salting-in/salting-out ions be classified as chaotropes/kosmotropes? *J. Phys. Chem. B* **2010**, *114*, 643–650. [CrossRef]
30. Zhang, Y.; Furyk, S.; Sagle, L.B.; Cho, Y.; Bergbreiter, D.E.; Cremer, D.E. Effects of Hofmeister Anions on the LCST of PNIPAM as a Function of Molecular Weight. *J. Phys. Chem. C* **2007**, *111*, 8916–8924. [CrossRef]
31. Mittal, N.; Benselfelt, T.; Ansari, F.; Gordeyeva, K.; Roth, S.V.; Wågberg, L.; Söderberg, L.D. Ion-Specific Assembly of Strong, Tough, and Stiff Biofibers. *Angew. Chem. Int. Ed.* **2019**, *58*, 18562–18569. [CrossRef]

32.	Cray, J.A.; Russell, J.T.; Timson, D.J.; Singhal, R.S.; Hallsworth, J.E. A universal measure of chaotropicity and kosmotropicity. *Environ. Microbiol.* **2013**, *15*, 287–296. [CrossRef] [PubMed]

33.	Gibb, B.C. Abiogenesis and the reverse Hofmeister effect. *Nat. Chem.* **2018**, *10*, 797–798. [CrossRef] [PubMed]

34.	Cockell, C.S.; McLean, C.M.; Perera, L.; Aka, S.; Stevens, A.; Dickinson, A.W. Growth of Non-Halophilic Bacteria in the Sodium-Magnesium-Sulfate-Chloride Ion System: Unravelling the Complexities of Ion Interactions in Terrestrial and Extraterrestrial Aqueous Environments. *Astrobiology* **2020**, *20*, 944–955. [CrossRef] [PubMed]

35.	Heinz, J.; Rambags, V.; Schulze-Makuch, D. Physicochemical Parameters Limiting Growth of *Debaryomyces hansenii* in Solutions of Hygroscopic Compounds and Their Effects on the Habitability of Martian Brines. *Life* **2021**, *11*, 1194. [CrossRef]

36.	Ball, P.; Hallsworth, J.E. Water structure and chaotropicity: Their uses, abuses and biological implications. *Phys. Chem. Chem. Phys.* **2015**, *17*, 8297–8305. [CrossRef]

37.	Dos Santos, A.P.; Diehl, A.; Levin, Y. Surface Tensions, Surface Potentials, and the Hofmeister Series of Electrolyte Solutions. *Langmuir* **2010**, *26*, 10778–10783. [CrossRef] [PubMed]

38.	Baer, M.D.; Pham, V.T.; Fulton, J.L.; Schenter, G.K.; Balasubramanian, M.; Mundy, C.J. Is Iodate a Strongly Hydrated Cation? *J. Phys. Chem. Lett.* **2011**, *2*, 2650–2654. [CrossRef]

39.	Sharma, B.; Chandra, A. Born–Oppenheimer Molecular Dynamics Simulations of a Bromate Ion in Water Reveal Its Dual Kosmotropic and Chaotropic Behavior. *J. Phys. Chem. B* **2018**, *122*, 2090–2101. [CrossRef]

40.	Millero, F.J. Molal volumes of electrolytes. *Chem. Rev.* **1971**, *71*, 147–176. [CrossRef]

41.	Collins, K.D. Ions from the Hofmeister series and osmolytes: Effects on proteins in solution and in the crystallization process. *Methods* **2004**, *34*, 300–311. [CrossRef]

42.	Collins, K.D. The behavior of ions in water is controlled by their water affinity. *Q. Rev. Biophys.* **2019**, *52*, E11. [CrossRef] [PubMed]

43.	Padova, J. Solvation Approach to Ion Solvent Interaction. *J. Chem. Phys.* **1964**, *40*, 691–694. [CrossRef]

44.	Mazzini, V.; Craig, V.S.J. What is the fundamental ion-specific series for anions and cations? Ion specificity in standard partial molar volumes of electrolytes and electrostriction in water and non-aqueous solvents. *Chem. Sci.* **2017**, *8*, 7052–7065. [CrossRef] [PubMed]

45.	Harned, H.S.; Owen, B.B.; King, C. *The Physical Chemistry of Electrolytic Solutions*; Reinhold Publishing Corporation: New York, NY, USA, 1943.

46.	Falkenhagen, H.; Vernon, E. The quantitative limiting law for the viscosity of simple strong electrolytes. *Physik. Z.* **1932**, *33*, 140.

47.	Schwierz, N.; Horinek, D.; Sivan, U.; Netz, R.R. Reversed Hofmeister series—The rule rather than the exception. *Curr. Opin. Colloid Interface Sci.* **2016**, *23*, 10–18. [CrossRef]

48.	Collins, K.D. Charge Density-Dependent Strength of Hydration and Biological Structure. *Biophys. J.* **1997**, *72*, 65–76. [CrossRef] [PubMed]

49.	Haynes, W.M.; Lide, D.R.; Bruno, T.J. *CRC Handbook of Chemistry and Physics*; CRC press: Boca Raton, FL, USA, 2016.

50.	Eysel, H.H.; Lipponer, K.G.; Oberle, C.; Zahn, I. Raman intensities of liquids: Absolute scattering activities and electro-optical parameters of the halate ions ClO_3^-, BrO_3^-, and IO_3^- in aqueous solutions. *Spectrochim. Acta Part Mol. Spectrosc.* **1992**, *48*, 219–224. [CrossRef]

51.	Li, M.; Zhuang, B.; Lu, Y.; Wang, Z.G.; An, L. Accurate Determination of Ion Polarizabilities in Aqueous Solutions. *J. Phys. Chem. B* **2017**, *121*, 6416–6424. [CrossRef]

52.	Oberle, C.; Eysel, H.H. Ab initio calculations for some oxo-anions of chlorine, bromine and iodine. *J. Mol. Struct. THEOCHEM* **1993**, *280*, 107–115. [CrossRef]

53.	Rabek, J.F. *Experimental Methods in Polymer Chemistry: Physical Principles and Applications*; John Wiley & Sons Ltd.: Hoboken, NJ, USA, 1991.

54.	Robinson, R.A.; Stokes, R.H. Tables of osmotic and activity coefficients of electrolytes in aqueous solution at 25 °C. *Trans. Faraday Soc.* **1949**, *45*, 612–624. [CrossRef]

55.	Durig, J.R.; Bonner, O.; Breazeale, W. Raman studies of iodic acid and sodium iodate. *J. Phys. Chem.* **1965**, *69*, 3886–3892. [CrossRef]

56.	Marcus, Y. Electrostriction in electrolyte solutions. *Chem. Rev.* **2011**, *111*, 2761–2783. [CrossRef] [PubMed]

57.	Marcus, Y.; Hefter, G. Standard partial molar volumes of electrolytes and ions in nonaqueous solvents. *Chem. Rev.* **2004**, *104*, 3405–3452. [CrossRef] [PubMed]

58.	Hamann, S.; Lim, S. The volume change on ionization of weak electrolytes. *Aust. J. Chem.* **1954**, *7*, 329–334. [CrossRef]

59.	Lo Nostro, P.; Ninham, B.W.; Milani, S.; Lo Nostro, A.; Pesavento, G.; Baglioni, P. Hofmeister effects in supramolecular and biological systems. *Biophys. Chem.* **2006**, *124*, 208–213. [CrossRef] [PubMed]

60.	Parsons, D.F.; Boström, M.; Lo Nostro, P.; Ninham, B.W. Hofmeister effects: Interplay of hydration, nonelectrostatic potentials, and ion size. *Phys. Chem. Chem. Phys.* **2011**, *13*, 12352–12367. [CrossRef]

61.	Lewis, G.N.; Randall, M.; Pitzer, K.S.; Brewer, L. *Thermodynamics*; Courier Dover Publications: Mineola, NY, USA, 2020.

62.	Millero, F.J. The apparent and partial molal volume of aqueous sodium chloride solutions at various temperatures. *J. Phys. Chem.* **1970**, *74*, 356–362. [CrossRef]

63.	Roy, M.N.; De, P.; Sikdar, P.S. Physicochemical study of solution behaviour of alkali metal perchlorates prevailing in *N,N*-Dimethyl Formamide with the manifestation of ion solvation consequences. *J. Mol. Liq.* **2015**, *204*, 243–247. [CrossRef]

64. Tomaš, R.; Kinart, Z.; Tot, A.; Papović, S.; Teodora Borović, T.; Vraneš, M. Volumetric properties, conductivity and computation analysis of selected imidazolium chloride ionic liquids in ethylene glycol. *J. Mol. Liq.* **2022**, *345*, 118178. [CrossRef]

65. Shekaari, H.; Jebali, F. Densities, Viscosities, Electrical Conductances, and Refractive Indices of Amino Acid + Ionic Liquid ([BMIm]Br) + Water Mixtures at 298.15 K. *J. Chem. Eng. Data* **2010**, *55*, 2517–2523. [CrossRef]

66. Marcus, Y. On the intrinsic volumes of ions in aqueous solutions. *J. Sol. Chem.* **2010**, *39*, 1031–1038. [CrossRef]

67. Pedersen, T.G.; Dethlefsen, C.; Hvidt, A. Volumetric properties of aqueous solutions of alkali halides. *Carlsberg Res. Commun.* **1984**, *49*, 445–455. [CrossRef]

68. Cox, W.; Wolfenden, J. The viscosity of strong electrolytes measured by a differential method. *Proc. Roy. Soc. A* **1934**, *145*, 475–488. [CrossRef]

69. Jones, G.; Dole, M. The viscosity of aqueous solutions of strong electrolytes with special reference to barium chloride. *J. Am. Chem. Soc.* **1929**, *51*, 2950–2964. [CrossRef]

70. Jiang, J.; Sandler, S.I. A New Model for the Viscosity of Electrolyte Solutions. *Ind. Eng. Chem. Res.* **2003**, *42*, 6267–6272. [CrossRef]

71. Horvath, A.L.; Horwood, E. *Handbook of Aqueous Electrolyte Solutions*; Halsted Press: Sydney, Australia, 1985.

72. Patil, R.S.; Shaikh, V.R.; Patil, P.D.; Borse, A.U.; Patil, K.J. The viscosity B and D coefficient (Jones–Dole equation) studies in aqueous solutions of alkyltrimethylammonium bromides at 298.15 K. *J. Mol. Liq.* **2014**, *200*, 416–424. [CrossRef]

73. Mitchell, D.J.; Ninham, B.W. Range of the Screened Coulomb Interaction in Electrolytes and Double Layer Problems. *Chem. Phys. Lett.* **1978**, *53*, 397–399. [CrossRef]

74. Kékicheff, P.; Ninham, B.W. The Double-Layer Interaction in Asymmetric Electrolytes. *EPL* **1990**, *12*, 471–477. [CrossRef]

75. Nylander, T.; Kékicheff, P.; Ninham, B.W. The Effect of Solution Behavior of Insulin on Interactions between Adsorbed Layers of Insulin. *J. Colloid Interface Sci.* **1994**, *164*, 136–150. [CrossRef]

76. Robinson, R.A.; Stokes, R.H. *Electrolyte Solutions*; Butterworths Scientific Publications: London, UK, 1959.

77. Poiseuille, J.L.M. Experimental investigations on the flow of liquids in tubes of very small diameter. *Ann. Chim. Phys.* **1847**, *21*, 76.

78. Partington, J.R. *A History of Chemistry*; Martino Fine Books: Eastford, CT, USA, 1961; Volume 3.

79. Tamamushi, R. Estimation of Individual Ionic Activity Coefficients from Conductivity Data on Strong Electrolytes in Dilute Aqueous Solutions. *Bull. Chem. Soc. Jpn.* **1974**, *47*, 1921–1926. [CrossRef]

80. Tamamushi, R. A Method for Determining the Degree of Dissociation of Symmetrical Associated Electrolytes from the Conductivity and Activity Data. *Bull. Chem. Soc. Jpn.* **1975**, *48*, 705–706. [CrossRef]

81. Onsager, L.; Fuoss, R.M. Irreversible Processes in Electrolytes. Diffusion, Conductance and Viscous Flow in Arbitrary Mixtures of Strong Electrolytes. *J. Phys. Chem.* **1932**, *36*, 2689–2778. [CrossRef]

82. Fuoss, R.M.; Hsia, K.L. Association of 1-1 salts in water. *Proc. Natl. Acad. Sci. USA* **1967**, *57*, 1550–1557. [CrossRef]

83. Fernandez-Prini, R.; Justice, J.C. Evaluation of the solubility of electrolytes from conductivity measurements. *Pure Appl. Chem.* **1984**, *56*, 541–547. [CrossRef]

84. Williams, J.W.; Falkenhagen, H. The Interionic Attraction Theory of Electrical Conductance. *Chem. Rev.* **1929**, *6*, 317–345. [CrossRef]

85. Ninham, B.W.; Lo Nostro, P. *Molecular Forces and Self Assembly: In Colloid, Nano Sciences and Biology*; Cambridge University Press: Cambridge, UK, 2010.

86. Marcus, Y. Ionic radii in aqueous solution. *Chem. Rev.* **1988**, *88*, 1475–1498. [CrossRef]

87. De Feijter, J.A.; Benjamins, J.; Veer, F.A. Ellipsometry as a tool to study the adsorption behavior of synthetic and biopolymers at the air–water interface. *Biopolym. Orig. Res. Biomol.* **1978**, *17*, 1759–1772. [CrossRef]

88. Ball, V. Hofmeister Effects of Monovalent Sodium Salts in the Gelation Kinetics of Gelatin. *J. Phys. Chem. B* **2019**, *123*, 8405–8410. [CrossRef]

89. Born, M.; Wolf, E. *Principles of optics: Electromagnetic theory of propagation, interference and diffraction of light*; Cambridge University Press: Cambridge, UK, 1999.